Biochemical and Biophysical Research Communications 683 (2023) 149106

Contents lists available at ScienceDirect

Biochemical and Biophysical Research Communications

journal homepage: www.elsevier.com/locate/ybbrc

Apolipoprotein E genotype-dependent accumulation of amyloid β in *APP*-knock-in mouse model of Alzheimer's disease

Yoshiko Takebayashi [a], Yu Yamazaki [a,*], Hidetada Yamada [a], Kyosuke Yazawa [a,b], Masahiro Nakamori [a], Takashi Kurashige [c], Hiroyuki Morino [d], Tetsuya Takahashi [e], Yusuke Sotomaru [f], Hirofumi Maruyama [a]

[a] Department of Clinical Neuroscience and Therapeutics, Graduate School of Biomedical and Health Sciences, Hiroshima University, Hiroshima, Japan
[b] Department of Pharmacotherapy, Graduate School of Biomedical and Health Sciences, Hiroshima University, Hiroshima, Japan
[c] Department of Neurology, National Hospital Organization Kure Medical Center and Chugoku Cancer Center, Kure, Japan
[d] Department of Medical Genetics, Tokushima University Graduate School of Biomedical Sciences, Tokushima, Japan
[e] Department of Rehabilitation, Faculty of Rehabilitation, Hiroshima International University, Higashihiroshima, Japan
[f] Natural Science Center for Basic Research and Development, Hiroshima University, Hiroshima, Japan

ARTICLE INFO

Keywords:
Alzheimer's disease
Amyloid-β
APP-knock-in mouse
Apolipoprotein E

ABSTRACT

Apolipoprotein E4 (APOE4), the strongest risk factor for late-onset Alzheimer's disease (AD), has been revealed to cause greater accumulation of extracellular amyloid β (Aβ) aggregates than does APOE3 in traditional transgenic mouse models of AD. However, concerns that the overexpression paradigm might have affected the phenotype remain. Amyloid precursor protein (*APP*)-knock-in (KI) mice, incorporating *APP* mutations associated with AD development, offer an alternative approach for overproducing pathogenic Aβ without needing overexpression of APP. Here, we present the results of comprehensive analyses of pathological and biochemical traits in the brains of *APP*-KI mice harboring *APP*-associated familial AD mutations ($APP^{NL\text{-}G\text{-}F/NL\text{-}G\text{-}F}$ mice) crossed with human *APOE*-KI mice. Immunohistochemical and biochemical analyses revealed the *APOE* genotype-dependent increase in Aβ pathology and glial activation, which was evident within 8 months in the mouse model. These results suggested that this mouse model may be valuable for investigating APOE pathobiology within a reasonable experimental time frame. Thus, this model can be considered in investigating the interaction between APOE and Aβ *in vivo,* which may not be addressed appropriately by using other transgenic mouse models.

1. Introduction

Alzheimer's disease (AD) is a devastating neurodegenerative disorder that results in a progressive cognitive decline, making it a significant contributor to dementia in the aging population [1]. With the global increase in the number of AD cases, comprehending its pathophysiology and developing effective treatments are imperative. The failure of many clinical trials in the prodromal and dementia stage of AD patients [2] highlights the need for therapeutic intervention in the preclinical phase of AD. To this end, preclinical AD models are essential as they allow amalgamation of insights from preclinical studies with human clinical research, fostering a deeper understanding of AD and advancing potential treatments [3].

One of the hallmarks of AD is the aggregation and accumulation of extracellular amyloid β (Aβ) in the brain [1]. To replicate these Aβ pathologies and contribute to our understanding of AD, preclinical mouse models have been created. Notably, transgenic mice expressing the amyloid precursor protein gene (*App*) with disease-associated mutations (e.g., 5XFAD-Tg: *App* transgenic mouse carrying five familial AD mutations, which exhibit significant Aβ deposition at 2 months of age [4]) have played a pivotal role in elucidating disease mechanisms and exploring therapeutic candidates [3]. However, it is crucial to acknowledge that transgenic models have limitations, including overexpression-related artifacts, unintended gene disruption, and variable expression patterns, which can diminish their relevance as preclinical AD models.

In response to these limitations, the development of human *APP*-knock-in (KI) mice represents a significant advancement. *APP*-KI mice

* Corresponding author. Department of Clinical Neuroscience and Therapeutics, Hiroshima University, Graduate School of Biomedical and Health Sciences 1-2-3 Kasumi, Minami-ku, Hiroshima, 734–8551, Japan.
E-mail address: yuyamazaki@hiroshima-u.ac.jp (Y. Yamazaki).

https://doi.org/10.1016/j.bbrc.2023.10.038
Received 17 September 2023; Accepted 9 October 2023
Available online 10 October 2023
0006-291X/

feature humanized mouse Aβ sequences with three familial AD mutations (Swedish, Iberian, and Arctic), introduced through a KI strategy [3,5]. This approach may mitigate the shortcomings associated with transgenic models. However, to comprehend the significance and utility of this model fully, comprehensive phenotypic evidence from diverse perspectives is required.

In this study, we aimed to investigate whether the genetic predisposition to exacerbated Aβ pathology, particularly that associated with apolipoprotein E4 (APOE4), a potent genetic risk factor for late-onset AD due to its role in accelerating Aβ accumulation [1], can be recapitulated in *APP*-KI mice. To this end, we analyzed pathological and biochemical traits in the brains of $APP^{NL\text{-}G\text{-}F/NL\text{-}G\text{-}F}$ mice crossed with human *APOE*-KI mice at different ages. The results revealed an *APOE* genotype-dependent accumulation of Aβ and glial activation in this mouse model, indicating the potential of *APP*-KI mice to replicate the *APOE4*-mediated exacerbation of Aβ pathology *in vivo*.

2. Material and methods

2.1. Animals

To generate double-gene KI mice, $APP^{NL\text{-}G\text{-}F/NL\text{-}G\text{-}F}$ (C57BL/6-App < tm3(NL-G-F)Tcs, RRID:IMSR_RBRC06344. C57BL/6J background) mice [3,5] were crossed with human *APOE3*-KI (B6; 129 Apoe < tm3(APOE3) sfu>/sfuRbrc, RRID:IMSR_RBRC03390. C57BL/6N background) or human *APOE4*-KI (B6; 129-Apoe < tm3(APOE4)sfu>/sfuRbrc RRID: IMSR_RBRC03418. C57BL/6N background) mice [6,7]; all the mice were provided by RIKEN BioResource Research Center (Tsukuba, Japan). Mice were housed in groups of two to four in individually ventilated cages under standard conditions (22 °C, 12-h light–dark cycle) with free access to food and water. Only double-KI mice homozygous for both genes were used in the experiments. The genetic background strain of the mice used in this experiment was mixed C57BL/6J; 6N. Details on the genotyping primers are described in sources cited above. All animal experiments were conducted with approximately equal numbers of males and females.

Animal experiments were conducted in accordance with the recommendations in the Guide for the Care and Use of Laboratory Animals of the Hiroshima University Animal Research Committee (No. A20-61-3).

2.2. Brain sample collection

Mice were euthanized after being anesthetized with 4% isoflurane for 2 min. The mice were then perfused intracardially with saline solution, and the right hemisphere was dissected into cortical and hippocampal regions, which were stored at −80 °C until further analysis. The left hemisphere was fixed in 4% paraformaldehyde for 3 days and then paraffinized.

2.3. Western blotting

Brain lysates for western blotting were prepared separately for the cortex and hippocampus of the right hemisphere, as described previously [8]. A 30-μg aliquot of protein from each sample was separated on 10% sodium dodecyl sulfate–polyacrylamide gels and electrophoretically transferred to ClearTrans SP polyvinylidene fluoride membranes (FUJIFILM Wako Pure Chemical Corporation, Osaka, Japan). Nonspecific binding sites on the membranes were blocked by incubation with EveryBlot Blocking Buffer (12010020, Bio-Rad, Hercules, CA, USA) for 10 min. The membranes were incubated for 1 h with the following primary antibodies: anti-APOE (1:500; ab183597, abcam, Cambridge, UK) and anti-α-tubulin (1:500,000; 66031-1-Ig, Proteinate, San Diego, CA, USA). Next, the membranes were incubated for 1 h with specific horseradish-peroxidase (HRP)-conjugated secondary antibodies (1:10,000). Protein expression was quantified from the band density using ImageJ software (National Institutes of Health, Bethesda, MD, USA) and normalized against the expression level of α-tubulin.

2.4. Enzyme-linked immunosorbent assay (ELISA)

Soluble materials from the cerebral cortex and hippocampus from the right hemisphere of the mouse were dissolved in tris-buffered saline (TBS), and insoluble materials were dissolved in 6 M guanidine-HCl solution (GuHCl), separately, as previously described [9], with a few modifications. Briefly, the frozen brain tissue was first homogenized in 1100 μl (cortex) and 450 μl (hippocampus) of TBS containing protease inhibitor cocktail (11697498001, Roche Diagnostics, Basel, Switzerland). The lysate was subject to centrifugation (200,000×*g* for 20 min at 4 °C) with a TLA-100.3 rotor (349481, Beckman Coulter Life Science, Brea, CA, USA) in an Optima MAX-XP centrifuge (393315, Beckman Coulter Life Science). The supernatant was defined as the TBS-soluble fraction, and 6 M GuHCl was added to yield a 0.5-M (final concentration) solution, which was stored at −80 °C until application in ELISA. The remaining pellet was added to the same volume of 6 M GuHCl as above, incubated for 1 h at room temperature, and homogenized. The lysate was centrifuged (200,000×*g* for 20 min at 25 °C). The supernatant was defined as the insoluble (GuHCl-soluble) fraction, and an 11-fold volume of TBS was added to the supernatant and stored at −80 °C until application in ELISA. The levels of Aβ42 and Aβ40 were measured using ELISA kits (290–62601 and 294–62501, respectively; FUJIFILM Wako Pure Chemical Corporation) according to the manufacturer's instructions. The obtained Aβ levels were normalized to the weight of the cortex and hippocampus, respectively.

2.5. Immunohistochemistry (IHC)

IHC for Aβ42, Aβ40, and glial fibrillary acidic protein (GFAP) was conducted using an automated system (Dako Autostainer Link 48, AS48030, DAKO, Santa Clara, CA, USA) with EnVision FLEX (K8000, DAKO) on 10-μm-thick formalin-fixed coronal brain paraffin sections. We performed antigen retrieval for Aβ42 and Aβ40 for 5 min using formic acid. Heat-induced epitope retrieval was performed for GFAP with the FLEX TRS High-pH Retrieval Buffer (DAKO) for 20 min. After peroxidase blocking for 20 min, the slides were blocked in Protein Block Serum-Free Reagent (X0909, DAKO) for 20 min. Thereafter, rabbit anti-human Aβ42 (1:200; 18582, IBL, Gunma, Japan), rabbit anti-human Aβ40 (1:100; 18580, IBL), and rabbit anti-GFAP (1:1000; AB5804, Sigma-Aldrich, St Louis, MO, USA) were applied for 120 min. The FLEX + Rabbit EnVision System was used for detection for 30 min. DAB chromogen was then applied for 10 min for Aβ42 and Aβ40 and for 1 min for GFAP. IHC for ionized calcium-binding adapter protein 1 (IBA1) was performed manually rather than using the autostainer. After antigen retrieval using 0.01 M citric acid (pH 6.0), the slides were microwaved for 10 min. The endogenous peroxidase was blocked with 3% hydrogen peroxide for 30 min. The slides were blocked in Protein Block Serum-Free Reagent for 20 min. Thereafter, rabbit anti-IBA1 (1:1000; 019–19741, Wako) was applied at 4 °C overnight. Next, the slides were incubated with HRP-polymer secondary antibody (EnVision+/HRP, Rabbit; K4003, DAKO) for 30 min. Target proteins were visualized after incubation with the peroxidase substrate DAB (SK 4100, Vector Laboratories, Newark, CA, USA) for 4 min. All slides were counterstained with hematoxylin for 1 min.

2.6. Quantitative assessment of neuropathological changes

We selected four sections per paraffin-block, at 450-μm intervals, starting from the section where the CA1 region of the hippocampus begins to be seen, and performed neuropathological assessment in a genotype-blinded manner, as follows [10]. We created panoramic images of each slide under the 10 × objective lens of a BX43 Olympus microscope with a DP74 digital camera microscope, using cellSens

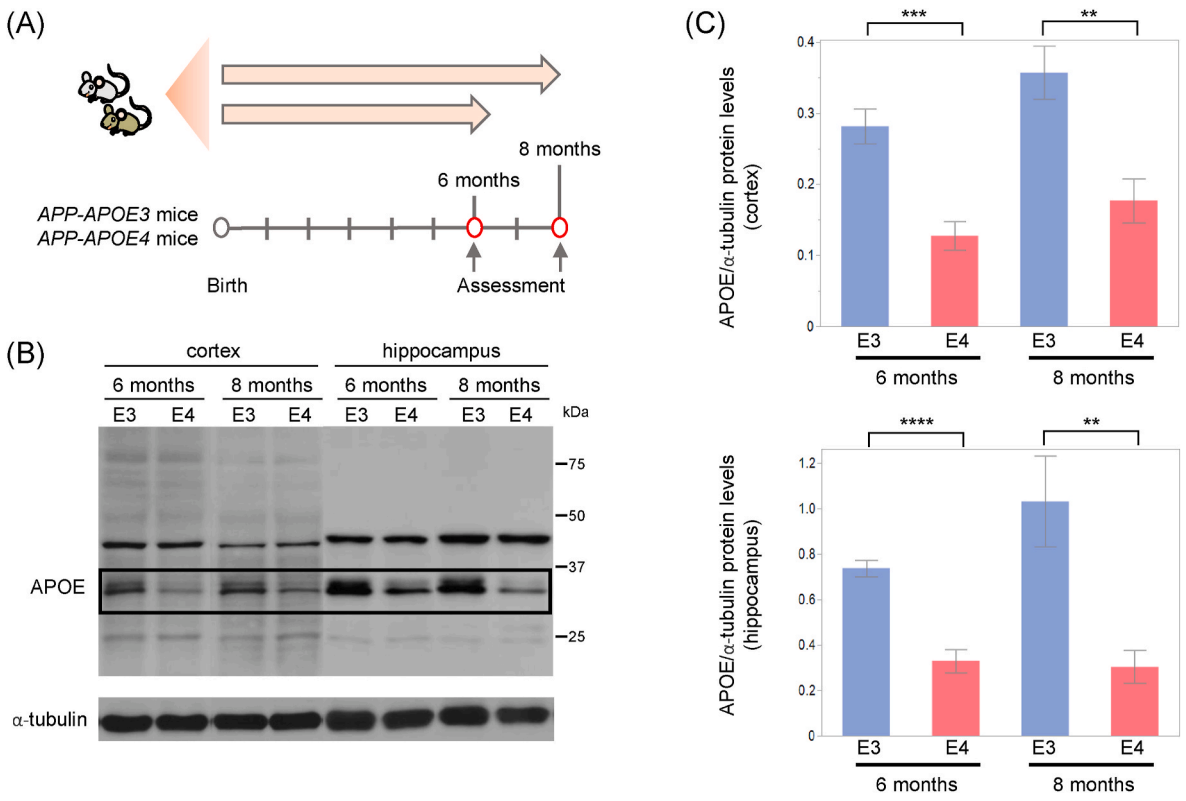

Fig. 1. Apolipoprotein E (APOE) protein levels in *APP-APOE4* mice are lower than in *APP-APOE3* mice.
(A) Timeline for assessment of APP$^{NL\text{-}G\text{-}F/NL\text{-}G\text{-}F}$/human APOE3(E4) (*APP-APOE3* [*APOE4*]) mice. (B) Western blot for cortical and hippocampal lysates of 6- and 8-month-old *APP-APOE3* (*APOE4*) mice with antibodies against APOE and α-tubulin. (C) Band density was standardized against the density of α-tubulin. The levels were compared between 6- and 8-month-old *APP-APOE3* (blue) and *APP-APOE4* (red) mice, using Student's *t*-test (means ± S.E.; n = 6–7; **p < 0.01, ***p < 0.001, ****p < 0.0001). Abbreviations: E3, *APP-APOE3*; E4, *APP-APOE4*. (For interpretation of the references to colour in this figure legend, the reader is referred to the Web version of this article.)

software (Olympus, Japan). We determined the thresholds of the positive immunoreactive area for use as default levels and adjusted minor parameters to optimize the positive immunoreactive area in each slide. We then measured the area of the brain subregion (cortex and hippocampus) as well as each immunoreactive area within the subregion in each slide and calculated the percentage of immunoreactive area per antibody using the cellSens Dimension software (Olympus) as well as the average of the percentage of each immunoreactive area of the four sections per mouse.

2.7. Statistical analysis

The available data were compared between APP$^{NL\text{-}G\text{-}F/NL\text{-}G\text{-}F}$/human APOE3 (*APP-APOE3*) and APP$^{NL\text{-}G\text{-}F/NL\text{-}G\text{-}F}$/human APOE4 (*APP-APOE4*) mice. Histological analysis and ELISA data were also compared between 6- and 8-month-old mice. Statistical significance was determined using Student's *t*-test and was set at $p < 0.05$. All analyses were performed using JMP 16.0 (SAS Institute, Inc., Cary, NC, USA).

3. Results

3.1. APOE genotype-dependent changes in brain APOE levels in APP-APOE-KI mice

To examine whether the *APOE4*-mediated exacerbation of Aβ pathology was recapitulated in *APP*-KI mice, we created and assessed *APP-APOE* mice by crossing APP$^{NL\text{-}G\text{-}F/NL\text{-}G\text{-}F}$ mice with human *APOE3* or *APOE4*-KI mice. As a result, we generated APP$^{NL\text{-}G\text{-}F/NL\text{-}G\text{-}F}$/human APOE3 mice, referred to as *APP-APOE3*, and APP$^{NL\text{-}G\text{-}F/NL\text{-}G\text{-}F}$/human APOE4 mice, referred to as *APP-APOE4* mice. The pathobiology related to APOE, within the context of Aβ pathology, was subsequently assessed both pathologically and biochemically in these mouse models at 6 and 8 months of age (Fig. 1A).

Since the level of APOE4 is lower than that of APOE3 in human brains [11], we first examined whether these amounts also differed between *APP-APOE3* and *APP-APOE4* mice. As anticipated, we observed that the amounts of APOE in both the cortex and hippocampus were lower in *APP-APOE4* mice than in *APP-APOE3* mice, at both 6 and 8 months of age (Fig. 1B and C).

3.2. APOE genotype-dependent changes in Aβ accumulation in APP-APOE-KI mice

As APOE4 has been shown to drive Aβ accumulation during aging in humans [1], we next examined whether *APOE4*-mediated exacerbation of Aβ pathology was also evident in *APP*-KI mice. To address this, we assessed the Aβ42 and Aβ40 plaque burden in 6- and 8-month-old *APP-APOE3* and *APP-APOE4* mice through IHC (Fig. 2A). We found that accumulation of Aβ42 and Aβ40 in the brain parenchyma had already been initiated by 6 months of age. Notably, the amount of Aβ plaques was higher in *APP-APOE4* mice than in *APP-APOE3* mice, but this significant difference was only observed at 8 months of age, in both the cortex and the hippocampus. As such, Aβ accumulation was seen to increase progressively with age, particularly in *APP-APOE4* mice (Fig. 2B).

To confirm the differences in Aβ accumulation observed through IHC between *APP-APOE3* and *APP-APOE4* further, we quantified the levels of Aβ42 and Aβ40 in brain homogenates from 6- and 8-month-old mice, using ELISA (Fig. 2C). Consistent with the Aβ accumulation patterns identified via IHC, we found that the Aβ42 and Aβ40 levels in the GuHCl-

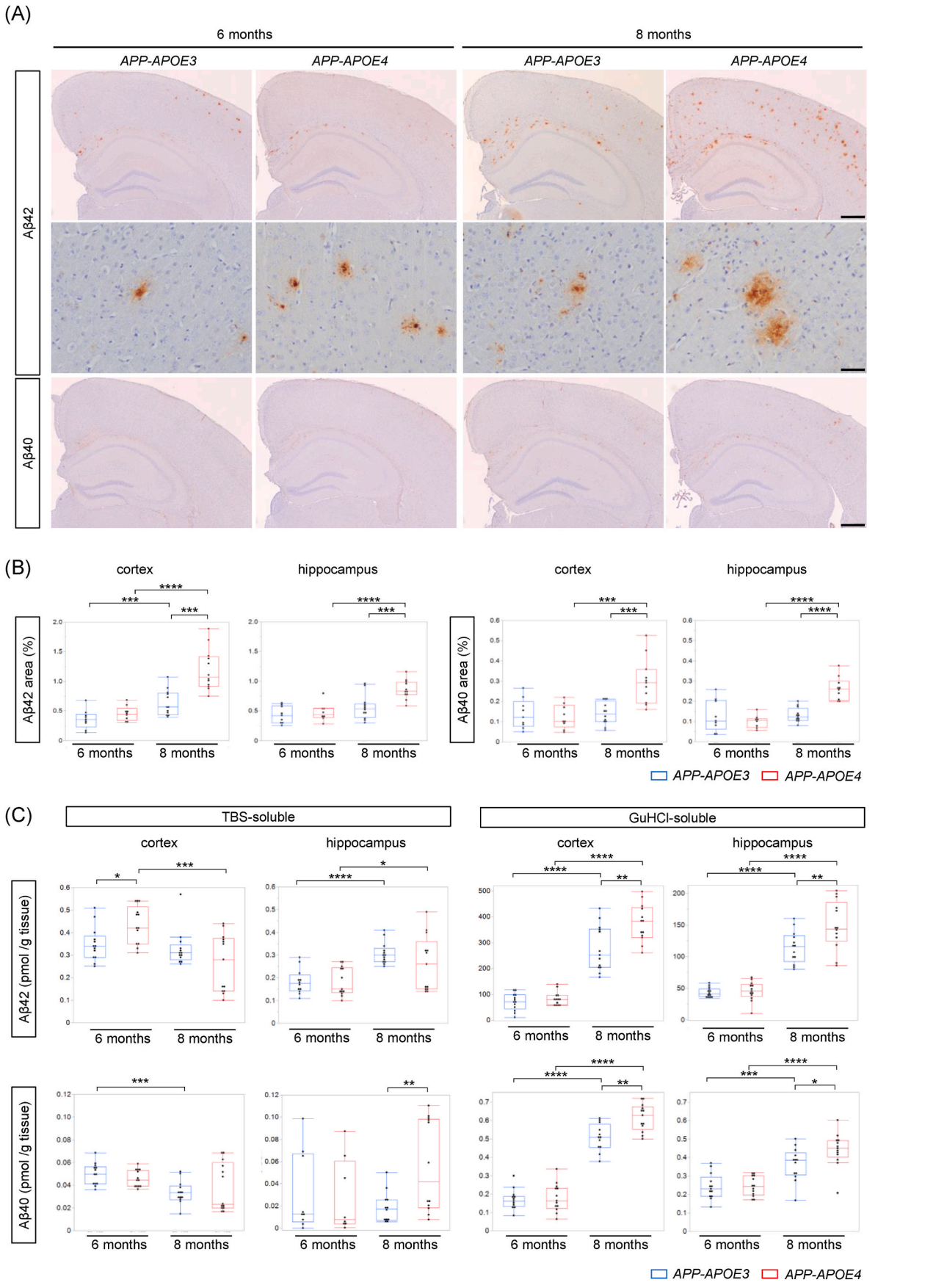

(caption on next page)

Fig. 2. Pathological and biochemical analysis of amyloid beta (Aβ) in 6- and 8-month-old *APP-APOE3* (*APOE4*) mice.
(A) Microscopic images of Aβ42 and Aβ40 immunoreactivity in the cortex and hippocampus of *APP-APOE3* (*APOE4*) mice. Scale bars = 500 μm (upper panels of Aβ42 and Aβ40), 50 μm (lower panels of Aβ42 (cortex)). (B) Percentage of area positive for anti-Aβ42 and anti-Aβ40 antibodies relative to the total area in the cortex and hippocampus of *APP-APOE3* (blue box plot) and *APP-APOE4* (red box plot) mice at 6 and 8 months of age (n = 8–12/group). (C) Biochemical levels of Aβ42 and Aβ40 in the cortex and hippocampus of *APP-APOE3* (blue box plot) and *APP-APOE4* (red box plot) mice, determined using ELISA. Aβ42 and Aβ40 levels in the tris-buffered saline (TBS)- and guanidine-HCl (GuHCl)-soluble fractions of 6- and 8-month-old mice were quantified. The middle line of the box plots indicates the median value for each group. Statistical significance was determined using Student's *t*-test (n = 9–13/group; *p < 0.05, **p < 0.01, ***p < 0.001, ****p < 0.0001). (For interpretation of the references to colour in this figure legend, the reader is referred to the Web version of this article.)

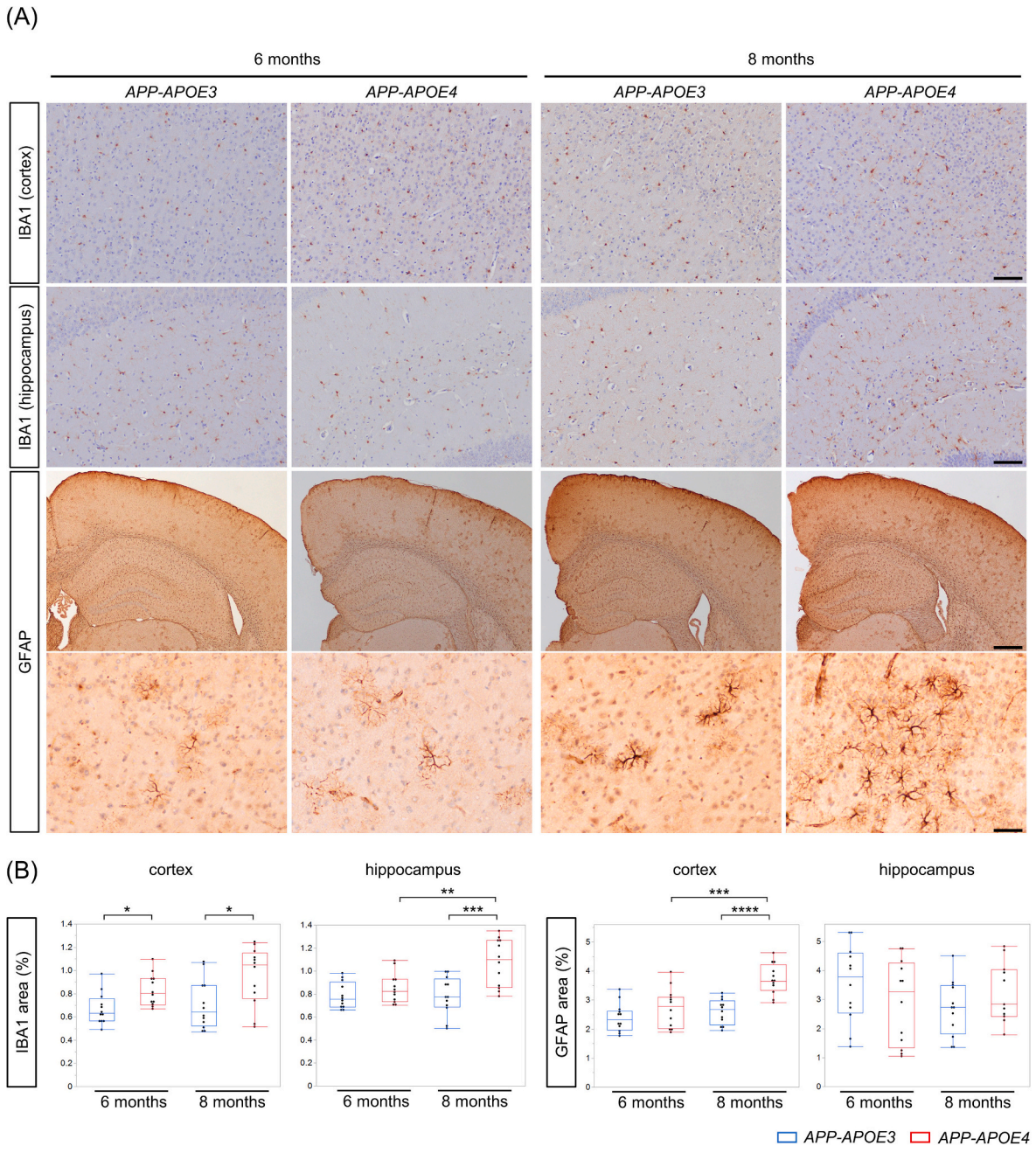

Fig. 3. Analysis of neuroinflammation in 6- and 8-month-old *APP-APOE3* (*APOE4*) mice.
(A) Microscopic images of glial fibrillary acidic protein (GFAP) and ionized calcium-binding adapter protein 1 (IBA1) immunoreactivity in the cortex and hippocampus of *APP-APOE3* (*APOE4*) mice at 6 and 8 months of age. Scale bars = 125 μm (IBA1), 500 μm (upper panels of GFAP), 50 μm (lower panels of GFAP (cortex)). (B) Percentage of area positive for IBA1 and GFAP antibodies relative to the total area in the cortex and hippocampus of *APP-APOE3* (blue box plot) and *APP-APOE4* (red box plot) mice at 6 and 8 months of age. The middle line of the box plots indicates the median value for each group. Statistical significance was determined using Student's t-test. (n = 11–12/group; *p < 0.05, **p < 0.01, ***p < 0.001, ****p < 0.0001). (For interpretation of the references to colour in this figure legend, the reader is referred to the Web version of this article.)

soluble fraction were higher in *APP-APOE4* mice than in *APP-APOE3* mice, in both the cortex and the hippocampus. In contrast, in the TBS-soluble fraction, no significant differences in Aβ levels were observed between *APP-APOE3* and *APP-APOE4* mice, except for elevated Aβ42 levels in the 6-month-old cortex of *APP-APOE4* mice and higher Aβ40 levels in the hippocampus of 8-month-old *APP-APOE4* mice. Collectively, these data suggested that *APP-APOE* mice demonstrated *APOE4*-mediated exacerbation of Aβ pathology, which became particularly pronounced at 8 months of age.

3.3. *APOE* genotype-dependent changes in glial activation in APP-APOE-KI mice

Astrocytes and microglia are two major cell types known to be activated in response to Aβ accumulation [1]. Thus, we investigated whether *APOE* genotype-dependent glial activation was observable in *APP*-KI mice by analyzing the percentage of GFAP- and IBA1-positive areas in the cortex and hippocampus of 6- and 8-month-old *APP-APOE3* and *APP-APOE4* mice. Representative images are provided in Fig. 3A. At 8 months of age, the percentage of positive area for IBA1 and GFAP in the cortex of *APP-APOE4* mice was higher than that in *APP-APOE3* mice, indicating increased glial activation in *APP-APOE4* mice. Similarly, in the hippocampus, the percentage of positive area for IBA1 was also higher in *APP-APOE4* mice than in *APP-APOE3* at 8 months of age. Interestingly, even in the cortex of 6-month-old *APP-APOE* mice, where *APOE4*-mediated exacerbation of Aβ pathology was not yet evident, the percentage of IBA1-positive area was higher in *APP-APOE4* mice than in *APP*-APOE3 mice. Collectively, these data suggested that *APP-APOE* mice demonstrate *APOE* genotype-dependent glial activation, which may even precede the differential regulation of Aβ accumulation by APOE genotypes.

4. Discussion

In this study, through the analysis of pathological and biochemical traits in the brains of $APP^{NL\text{-}G\text{-}F/NL\text{-}G\text{-}F}$ mice crossed with human *APOE*-KI mice, we found the following. First, *APOE4*-mediated exacerbation of Aβ pathology became particularly pronounced at 8 months of age in *APP*-KI mice. Second, *APOE* genotype-dependent glial activation preceded the differential regulation of Aβ accumulation by *APOE* genotypes in *APP*-KI mice. Finally, the level of brain APOE was lower in the presence of *APOE4* than in the presence of *APOE3* in these mice. Collectively, these results demonstrated an *APOE* genotype-dependent accumulation of Aβ and concurrent glial activation in this mouse model, underscoring its potential to replicate the *APOE4*-mediated exacerbation of Aβ pathology faithfully in an *in vivo* context. The observed decrease in the APOE level in the presence of *APOE4*, compared to that in the presence of *APOE3*, further supported the notion that this model faithfully recapitulates key APOE biology. This reduction in APOE4 levels was consistent with the phenomenon observed in individuals with AD [11], possibly mirroring the shift of the APOE4 pool co-deposited with amyloid plaques into the detergent-insoluble fraction [12].

In clear contrast to the increase in Aβ accumulation during aging, cortical soluble Aβ levels tended to exhibit a decline over time from 6 to 8 months of age in both *APP-APOE4* and *APP-APOE3* mice. Prior studies on 5XFAD mice have suggested that soluble Aβ, which forms before deposition of amyloid plaques, exists as highly toxic oligomers [13]. While the nature of the soluble Aβ quantified in our ELISA remains to be definitively established, using this mouse model at an age younger than 6 months for studies focusing on therapeutically targeting soluble Aβ (which is abundant before Aβ deposition) may be advisable, because numerous studies have linked Aβ-induced neurotoxicity to the soluble pool of Aβ42 [14,15].

Several limitations of this study need to be acknowledged. Firstly, we did not account for potential adverse effects of APOE4 in the context of vascular conditions in AD [16]. Furthermore, we did not consider potential differences in atherosclerosis due to varying genetic backgrounds in the mice [17]. Secondly, this study was conducted only at limited time points, specifically at 6 and 8 months of age. Lastly, we did not explore neuroinflammation with respect to Aβ-associated microglial activation, because we only examined the percentage of IBA1-positive area in the cortex and hippocampus. Thus, *APOE* genotype-dependent microglial activation observed in the 6-month-old mouse cortex might indicate strong Aβ-independent APOE4-related neuroinflammation [18]. Further investigations encompassing Aβ-associated neuroinflammation at various ages in this mouse model are warranted. Nonetheless, our study was significant in that it demonstrated the capability of *APP*-KI mice to replicate the *in vivo* exacerbation of Aβ pathology mediated by *APOE4* within a reasonable experimental time frame. As summarized in Table 1, this mouse model performed comparably to the transgenic mouse models that are widely used in AD and related dementia research, faithfully recapitulating key APOE pathobiology.

Table 1
Differences in the effects of the *APOE* genotype in the APOE: 5XFAD mouse and patient with AD, as compared to this mouse model.

	APOE genotype-dependent Aβ accumulation		APOE protein levels	Microglial activation
	Histopathology	Biochemistry		
APOE: 5XFAD mouse	E3<E4 [19,20] (4–7 M)	E3<E4 [19,20] (4–7 M)	E3>E4 [19] (2–6 M)	E3<E4 [21] (6 M)
Patient with AD	E3<E4 [22,23]	E3 = E4 [24]	E3>E4 [11]	E4 non carriers = E4 carriers [25]
This mouse model	E3<E4 (8 M)	E3<E4 (6 M)	E3>E4 (6–8 M)	E3<E4 (6–8 M)

APOE genotype-dependent biochemical differences regarding soluble Aβ42 are shown. The age at which differences in *APOE* genotype-dependent expression was detected is presented in parentheses.
Abbreviations: APOE, Apolipoprotein E; APOE: 5XFAD mouse, 5XFAD-Tg mouse crossed with human APOE3 (APOE4)-targeted replacement mouse; AD, Alzheimer's disease; Aβ, Amyloid-β; E3, Apolipoprotein E3; E4, apolipoprotein E4; M, months of age.

5. Conclusion

APOE genotype-dependent accumulation of Aβ and glial activation were observed in $APP^{NL\text{-}G\text{-}F/NL\text{-}G\text{-}F}$ mice. Since the KI approach is expected to alleviate the limitations associated with transgenic models, this model may be useful for addressing research inquiries that necessitate preclinical models recapitulating *APOE*-dependent accumulation of Aβ.

Funding sources

This work was funded by Takeda Science Foundation to TK and JSPS KAKENHI [grant number 20H03578] to YY.

Declaration of competing interest

The authors declare the following financial interests/personal relationships which may be considered as potential competing interests: Takashi Kurashige reports financial support was provided by Takeda Science Foundation.

Acknowledgments

We express our gratitude to Dr. Takashi Saito and Dr. Takaomi C. Saido (RIKEN Brain Science Institute, Japan) for providing the *APP*-KI mice, and Mitsubishi Chemical Corporation for providing the *APOE*-KI

mice. We would also like to express our gratitude to Dr. Koji Ikegami (Department of Anatomy and Developmental Biology, Graduate School of Biomedical and Health Sciences, Hiroshima University) for his kind attention to the use of the ultracentrifuge (Optima MAX-XP). We also thank Ms. Miwako Sasanishi and Ms. Yasuko Furuno (Department of Clinical Neuroscience and Therapeutics, Hiroshima University Graduate School of Biomedical and Health Sciences) and Ms. Kazuko Mihara and Ms. Miyuki Kiriki (Department of Clinical Research, National Hospital Organization Kure Medical Center and Chugoku Cancer Center) for their excellent technical assistance. Lastly, the authors are grateful to the Natural Science Center for Basic Research and Development, Hiroshima University, for providing access to their equipment during the preliminary phase of this project (NBARD-00014).

Appendix A. Supplementary data

Supplementary data to this article can be found online at https://doi.org/10.1016/j.bbrc.2023.10.038.

References

[1] Y. Yamazaki, N. Zhao, T.R. Caulfield, C.C. Liu, G. Bu, Apolipoprotein E and Alzheimer disease: pathobiology and targeting strategies, Nat. Rev. Neurol. 15 (2019) 501–518, https://doi.org/10.1038/s41582-019-0228-7.

[2] S. Asher, R. Priefer, Alzheimer's disease failed clinical trials, Life Sci. 306 (2022), 120861, https://doi.org/10.1016/j.lfs.2022.120861.

[3] H. Sasaguri, P. Nilsson, S. Hashimoto, K. Nagata, T. Saito, B. De Strooper, J. Hardy, R. Vassar, B. Winblad, T.C. Saido, APP mouse models for Alzheimer's disease preclinical studies, EMBO J. 36 (2017) 2473–2487, https://doi.org/10.15252/embj.201797397.

[4] H. Oakley, S.L. Cole, S. Logan, E. Maus, P. Shao, J. Craft, A. Guillozet-Bongaarts, M. Ohno, J. Disterhoft, L. Van Eldik, R. Berry, R. Vassar, Intraneuronal beta-amyloid aggregates, neurodegeneration, and neuron loss in transgenic mice with five familial Alzheimer's disease mutations: potential factors in amyloid plaque formation, J. Neurosci. 26 (2006) 10129–10140, https://doi.org/10.1523/jneurosci.1202-06.2006.

[5] T. Saito, Y. Matsuba, N. Mihira, J. Takano, P. Nilsson, S. Itohara, N. Iwata, T. C. Saido, Single App knock-in mouse models of Alzheimer's disease, Nat. Neurosci. 17 (2014) 661–663, https://doi.org/10.1038/nn.3697.

[6] H. Hamanaka, Y. Katoh-Fukui, K. Suzuki, M. Kobayashi, R. Suzuki, Y. Motegi, Y. Nakahara, A. Takeshita, M. Kawai, K. Ishiguro, M. Yokoyama, S.C. Fujita, Altered cholesterol metabolism in human apolipoprotein E4 knock-in mice, Hum. Mol. Genet. 9 (2000) 353–361, https://doi.org/10.1093/hmg/9.3.353.

[7] T. Mori, M. Kobayashi, T. Town, S.C. Fujita, T. Asano, Increased vulnerability to focal ischemic brain injury in human apolipoprotein E4 knock-in mice, J. Neuropathol. Exp. Neurol. 62 (2003) 280–291, https://doi.org/10.1093/jnen/62.3.280.

[8] H. Fujii, T. Takahashi, T. Mukai, S. Tanaka, N. Hosomi, H. Maruyama, N. Sakai, M. Matsumoto, Modifications of tau protein after cerebral ischemia and reperfusion in rats are similar to those occurring in Alzheimer's disease - hyperphosphorylation and cleavage of 4- and 3-repeat tau, J. Cerebr. Blood Flow Metabol. 37 (2017) 2441–2457, https://doi.org/10.1177/0271678x16668889.

[9] N. Iwata, H. Mizukami, K. Shirotani, Y. Takaki, S. Muramatsu, B. Lu, N.P. Gerard, C. Gerard, K. Ozawa, T.C. Saido, Presynaptic localization of neprilysin contributes to efficient clearance of amyloid-beta peptide in mouse brain, J. Neurosci. 24 (2004) 991–998, https://doi.org/10.1523/jneurosci.4792-03.2004.

[10] J. Kang, H. Watanabe, J. Shen, Protocols for assessing neurodegenerative phenotypes in Alzheimer's mouse models, STAR Protoc. 2 (2021), 100654, https://doi.org/10.1016/j.xpro.2021.100654.

[11] J. Poirier, Apolipoprotein E, cholesterol transport and synthesis in sporadic Alzheimer's disease, Neurobiol. Aging 26 (2005) 355–361, https://doi.org/10.1016/j.neurobiolaging.2004.09.003.

[12] K.R. Bales, F. Liu, S. Wu, S. Lin, D. Koger, C. DeLong, J.C. Hansen, P.M. Sullivan, S. M. Paul, Human APOE isoform-dependent effects on brain beta-amyloid levels in PDAPP transgenic mice, J. Neurosci. 29 (2009) 6771–6779, https://doi.org/10.1523/jneurosci.0887-09.2009.

[13] K.L. Youmans, S. Leung, J. Zhang, E. Maus, K. Baysac, G. Bu, R. Vassar, C. Yu, M. J. LaDu, Amyloid-β42 alters apolipoprotein E solubility in brains of mice with five familial AD mutations, J. Neurosci. Methods 196 (2011) 51–59, https://doi.org/10.1016/j.jneumeth.2010.12.025.

[14] M. Ohno, L. Chang, W. Tseng, H. Oakley, M. Citron, W.L. Klein, R. Vassar, J. F. Disterhoft, Temporal memory deficits in Alzheimer's mouse models: rescue by genetic deletion of BACE1, Eur. J. Neurosci. 23 (2006) 251–260, https://doi.org/10.1111/j.1460-9568.2005.04551.x.

[15] M.S. Durakoglugil, Y. Chen, C.L. White, E.T. Kavalali, J. Herz, Reelin signaling antagonizes beta-amyloid at the synapse, Proc. Natl. Acad. Sci. U. S. A. 106 (2009) 15938–15943, https://doi.org/10.1073/pnas.0908176106.

[16] Y. Yamazaki, C.C. Liu, A. Yamazaki, F. Shue, Y.A. Martens, Y. Chen, W. Qiao, A. Kurti, H. Oue, Y. Ren, Y. Li, T. Aikawa, Y. Cherukuri, J.D. Fryer, Y.W. Asmann, B.Y.S. Kim, T. Kanekiyo, G. Bu, Vascular ApoE4 impairs behavior by modulating gliovascular function, Neuron 109 (2021) 438–447, https://doi.org/10.1016/j.neuron.2020.11.019.

[17] Z. Su, Y. Li, J.C. James, M. McDuffie, A.H. Matsumoto, G.A. Helm, J.L. Weber, A. J. Lusis, W. Shi, Quantitative trait locus analysis of atherosclerosis in an intercross between C57BL/6 and C3H mice carrying the mutant apolipoprotein E gene, Genetics 172 (2006) 1799–1807, https://doi.org/10.1534/genetics.105.051912.

[18] M.P. Vitek, C.M. Brown, C.A. Colton, APOE genotype-specific differences in the innate immune response, Neurobiol. Aging 30 (2009) 1350–1360, https://doi.org/10.1016/j.neurobiolaging.2007.11.014.

[19] K.L. Youmans, L.M. Tai, E. Nwabuisi-Heath, L. Jungbauer, T. Kanekiyo, M. Gan, J. Kim, W.A. Eimer, S. Estus, G.W. Rebeck, E.J. Weeber, G. Bu, C. Yu, M.J. Ladu, APOE4-specific changes in Aβ accumulation in a new transgenic mouse model of Alzheimer disease, J. Biol. Chem. 287 (2012) 41774–41786, https://doi.org/10.1074/jbc.M112.407957.

[20] M. Cacciottolo, A. Christensen, A. Moser, J. Liu, C.J. Pike, C. Smith, M.J. LaDu, P. M. Sullivan, T.E. Morgan, E. Dolzhenko, A. Charidimou, L.O. Wahlund, M. K. Wiberg, S. Shams, G.C. Chiang, C.E. Finch, The APOE4 allele shows opposite sex bias in microbleeds and Alzheimer's disease of humans and mice, Neurobiol. Aging 37 (2016) 47–57, https://doi.org/10.1016/j.neurobiolaging.2015.10.010.

[21] G.A. Rodriguez, L.M. Tai, M.J. LaDu, G.W. Rebeck, Human APOE4 increases microglia reactivity at Aβ plaques in a mouse model of Aβ deposition, J. Neuroinflammation 11 (2014) 111, https://doi.org/10.1186/1742-2094-11-111.

[22] D.E. Schmechel, A.M. Saunders, W.J. Strittmatter, B.J. Crain, C.M. Hulette, S. H. Joo, M.A. Pericak-Vance, D. Goldgaber, A.D. Roses, Increased amyloid beta-peptide deposition in cerebral cortex as a consequence of apolipoprotein E genotype in late-onset Alzheimer disease, Proc. Natl. Acad. Sci. U. S. A. 90 (1993) 9649–9653, https://doi.org/10.1073/pnas.90.20.9649.

[23] T. Polvikoski, R. Sulkava, M. Haltia, K. Kainulainen, A. Vuorio, A. Verkkoniemi, L. Niinistö, P. Halonen, K. Kontula, Apolipoprotein E, dementia, and cortical deposition of beta-amyloid protein, N. Engl. J. Med. 333 (1995) 1242–1247, https://doi.org/10.1056/nejm199511093331902.

[24] M. Tachibana, M.L. Holm, C.C. Liu, M. Shinohara, T. Aikawa, H. Oue, Y. Yamazaki, Y.A. Martens, M.E. Murray, P.M. Sullivan, K. Weyer, S. Glerup, D.W. Dickson, G. Bu, T. Kanekiyo, APOE4-mediated amyloid-β pathology depends on its neuronal receptor LRP1, J. Clin. Invest. 129 (2019) 1272–1277, https://doi.org/10.1172/jci124853.

[25] A. Serrano-Pozo, A. Muzikansky, T. Gómez-Isla, J.H. Growdon, R.A. Betensky, M. P. Frosch, B.T. Hyman, Differential relationships of reactive astrocytes and microglia to fibrillar amyloid deposits in Alzheimer disease, J. Neuropathol. Exp. Neurol. 72 (2013) 462–471, https://doi.org/10.1097/NEN.0b013e3182933788.